REAL-TIME CHARACTERIZATION OF MIXED PLASTIC WASTE USING MACHINE LEARNING AND INFRARED SPECTROSCOPY

Shengli Jiang [a,1], Zhuo Xu [b], Medhvi Kamran [b], Stas Zinchik [b], Fei Long [b], Sidike Paheding [c], Armando G. McDonald [d], Søren Friis [e], Lasse Høgstedt [e], Ezra Bar-Ziv [b] and Victor M. Zavala [a]

[a] Department of Chemical Engineering, University of Wisconsin – Madison, Madison, Wisconsin 53706, United States

[b] Department of Mechanical Engineering, Michigan Technological University, Houghton, Michigan 49931, United States

[c] Department of Applied Computing, Michigan Technological University, Houghton, Michigan 49931, United States

[d] Department of Forest, Rangeland and Fire Sciences, University of Idaho, Moscow, Idaho 83844, United States

[e] NLIR ApS, Farum 3520, Denmark

We present a sensing framework that combines a convolutional neural network (CNN) and fast IR (infrared spectroscopy) for classifying mixed plastic waste (MPW) streams containing various types of plastic materials. Importantly, this type of spectral data can be collected in real-time; consequently, this method facilitates the high-throughput characterization of MPW. The proposed CNN architecture, which we call PlasticNet, employs a Gramian angular representation of the spectrum. We demonstrate that this 2-dimensional (2D) matrix representation highlights correlations between different frequencies (wavenumber) and significantly improves classification accuracy compared to the use of spectra alone (a 1D vector representation).

Keywords

Machine learning, Plastic waste, IR spectra, Classification, Real-time

Introduction

Plastics are inexpensive and long-lasting materials that can be easily shaped into a variety of products for a wide range of applications, including food packaging, construction, and electronics. As a result, plastics production has increased significantly over the past seven decades. Along with the rapid growth of plastic production, the rate of plastic recycling growth is also concerning. In particular, mixed plastic waste (MPW) has posed significant ecological and environmental challenges, but only 8.7% of it is recycled [1]. The majority of recycled plastics are downgraded to low-value products; for instance, high-density polyethylene (HDPE) used in milk jugs is frequently reprocessed into less expensive construction materials, such as plastic tables and chairs [2]. The low-value products significantly reduce the incentive to recycle municipal solid waste. Multiple types of plastic mixtures that are contaminated with other materials cannot be identified by an inefficient sorting system, which is the primary cause of the difficulties in recycling MPW [3].

Because the majority of municipal solid waste (MSW) is disposed of in landfills, new recycling methods (pyrolysis [4], plastic alloying [5], etc.) are being investigated; however, all of these solutions require an understanding of the composition of MPW, particularly the potential contaminants [6]. A single plastic component has been successfully identified using nondestructive techniques such as infrared (IR) spectroscopy, X-ray diffraction, and other methods [7, 8, 9, 10]. Among these techniques, IR spectroscopy has garnered particular interest due to its ability to identify plastic polymers with accuracy. However, IR spectra may be obscured for various reasons (i.e., they may contain systematic errors and noise), which can make spectral identification difficult.

Recently, deep learning techniques such as convolutional neural networks (CNNs) have been applied to the analysis of IR spectral data, as they show promise for improved prediction accuracy and noise tolerance [11]. CNNs can automatically extract and organize discriminative features directly from the raw data in a hierarchical fashion, without the need to precompute engineering-crafted features. Chen et al. used a one-dimensional (1D) CNN to analyze NIR spectra and obtained satisfactory outcomes [12].

Despite their high identification accuracies, these methods are unsuitable for industrial applications because they either require manual sample collection or have slow data collection rates. In industrial settings, MPW pellets are rapidly transported along a conveyor belt, necessitating real-time sorting at high data collection rates. Therefore, a production-ready MPW sorting system requires equipment for rapid data collection (also known as "online") and an effective identification algorithm. In addition, recent studies have only identified the signal of a single plastic composition in municipal solid waste. IR signals from MPW containing two or more

[1] Corresponding author: Victor M. Zavala (E-mail: zavalatejeda@wisc.edu).

plastic compositions may present additional difficulties for the CNN method.

In this paper, we summarize the results from our two previous papers [13, 14]. In the first work, we propose a computational framework to characterize plastic components of MPW by analyzing the attenuated total reflection-Fourier transform infrared spectroscopy (ATR-FTIR) spectra using CNNs. Experimental data was obtained by preparing small sheets of plastics of different shapes and used ATR-FTIR to scan sheets for 10 different types; this data collection approach mimics how rigid waste plastics are found in online processing of MPW streams. In the second work, we propose to use a fast mid infrated (MIR) spectrometer to enable online plastic component measurements (see Fig. 1). Specifically, the fast MIR spectrometer uses a solid-state crystal that can change its refractive index and polarization based on temperature and voltage [15, 16]. It can measure IR spectra in the range of 800-5000 cm^{-1} at a speed up to 400 Hz (S2050 2.0-5.0 μm Fiber Spectrometer, NLIR), with a resolution of 6 cm^{-1} (2048 pixels) and a sensitivity of 10 pW/nm. The experimental data was obtained by measuring small black plastic pellets colored with carbon black. Twelve different types of plastic, a binary blend, and a ternary blend were measured with a fast IR spectrometer at 200 Hz for a better signal-to-noise ratio. This data collection method mimicked the online MPW processing. We show that the combination of IR and CNN creates a powerful, inexpensive, and rapid method for analyzing the composition of plastic waste, which enables the recycling and reproduction of high-quality plastics in the future.

Experimental Data Collection and Preparation

The ATR-FTIR dataset studied included spectra for 10 different, commercially-available plastic materials (see Fig. 2). Specifically, these were butadiene styrene (ABS), acrylic (AC), polyethylene (PE), polyethylene terephthalate (PET), polybutadiene (BR), polycarbonate (PC), polyisoprene (PI), polystyrene (PS), polypropylene (PP), and polyvinyl chloride (PVC).

The MIR dataset studied included spectra for 12 commercially available plastic materials commonly found in the MPW (see Fig. 3). The following materials were considered: acrylonitrile ABS, high impact polystyrene (HIPS), nylon-12 (PA12), PE, PET, polylactic acid (PLA), poly(methyl methacrylate) (PMMA), polyoxymethylene (POM), PP, PS, PVC, and PC. Additionally, two plastic blends were used as samples. The binary blend consisted of ABS and PC in a 1:1 ratio, whereas the tertiary blend was comprised of PP, PE, and PS in a 1:1:1 ratio. Except for the PS samples, which contained blue pigments, every sample of plastic was black.

Data Processing

For each ATR-FTIR plastic sample, 70 spectra were obtained. Each spectrum had 4150 data points, where each point represents the intensity at a given wavenumber (cm^{-1}). Each spectrum is encoded in a vector in $\mathbb{R}^{4150}$. For each MIR plastic sample, 5000 spectra were acquired. Each spectrum had 1600 data points (encoded in a vector in $\mathbb{R}^{1600}$). All spectra were normalized to be in the range $[0,1]$ to facilitate the ML analysis:

$$\hat{x} = \frac{x - \min(X)}{\max(X) - \min(X)} \tag{1}$$

where x was the original vector (a raw spectrum), $\hat{x}$ was the normalized vector (a normalized spectrum), and X was a matrix obtained by stracking all original vectors. Similarly, by stacking all the normalized vectors, we obtained the normalized spectra matrix $\hat{X}$, which was randomly split into a training set and a test set.

The training set is the dataset used to fit the parameters of ML models during the learning process. The test set is an independent dataset used to evaluate the performance (accuracy) of the ML model. Thirty percent of the elements of the training set were chosen at random and utilized as the validation set for tuning the ML architecture. To verify the robustness and generalizability of the ML model, we used a 5-fold cross-validation method.

Computational Framework

The proposed framework incorporates a CNN architecture that we refer to as PlasticNet. PlasticNet can function as a 1D CNN because its architecture converts IR spectra to vectors (1D data objects). PlasticNet can also operate as a 2D CNN because the framework includes a Gramian angular fields method that transforms spectral vectors into GAF matrices (2D data objects). The framework also consists of saliency analysis techniques that enable us to comprehend the characteristics that CNNs look for in IR spectra when identifying plastic components.

1D CNN

The architecture of the proposed 1D CNN is shown in Fig. 4. 1D CNNs extract features from IR spectra by convolution and pooling operations. An IR vector was directly fed into the 1D CNN, which we refer to as PlasticNet (1D). It included four convolutional layers, two max-pooling layers, and three fully connected layers. Each convolutional layer had 64 filters of size 3, while the max-pooling layer had filters of size 2. Each fully connected layer had 64 nodes. The activation function is rectified linear unit (ReLU).

Gramian Angular Fields

Although the vector representation of IR spectra already provides a wealth of information, the correlations between different frequencies are not encoded in a clear manner. Recently, Gramian angular fields (GAF) have been used to map time-series objects into matrices to capture correlation structures; this data transformation technique has been demonstrated to improve classification accuracy when analyzed with 2D CNNs [17]. Our hypothesis is that the accuracy of predictions can be improved by applying a similar principle to IR spectra. GAF represents vectors in polar coordinates and transforms these angles into symmetric matrices using

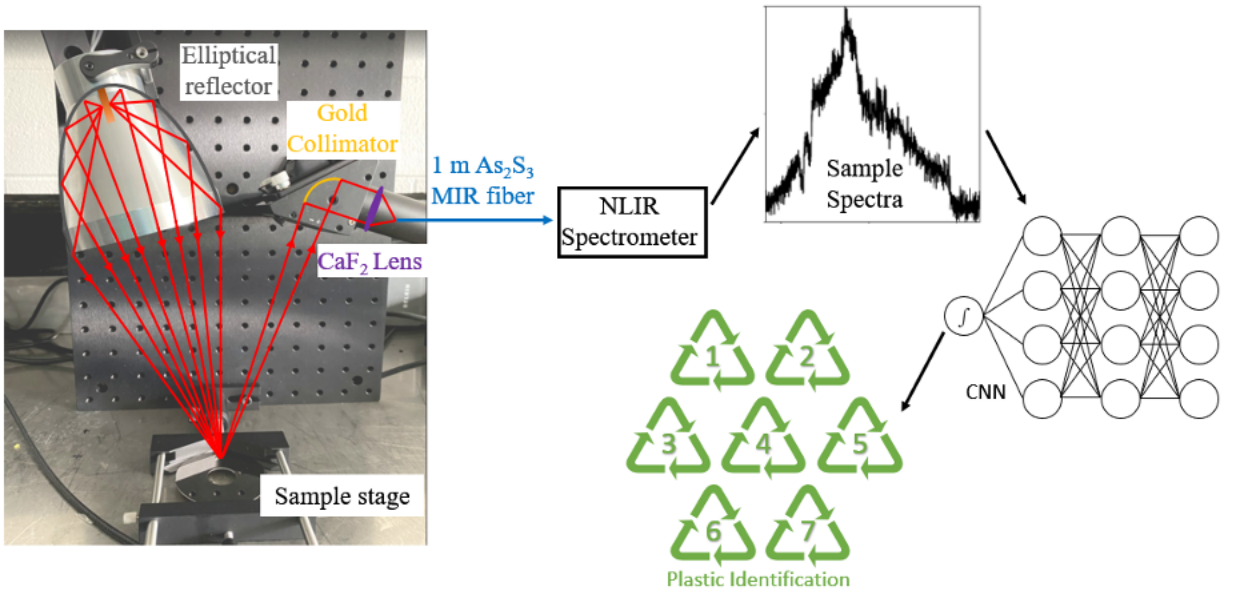

Figure 1: Experimental setup of the fast mid-infrared upconversion system.

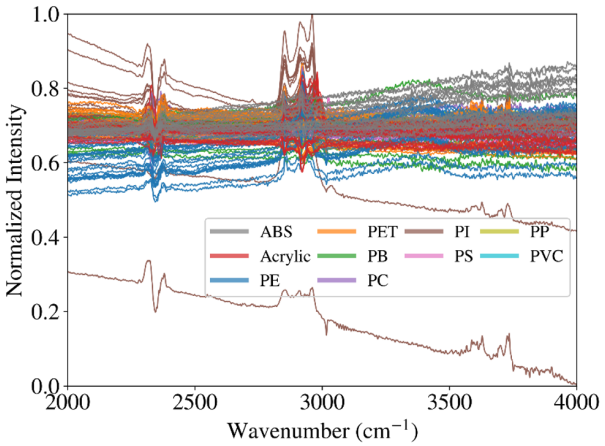

Figure 2: Normalized ATR-FTIR spectra of various plastic materials.

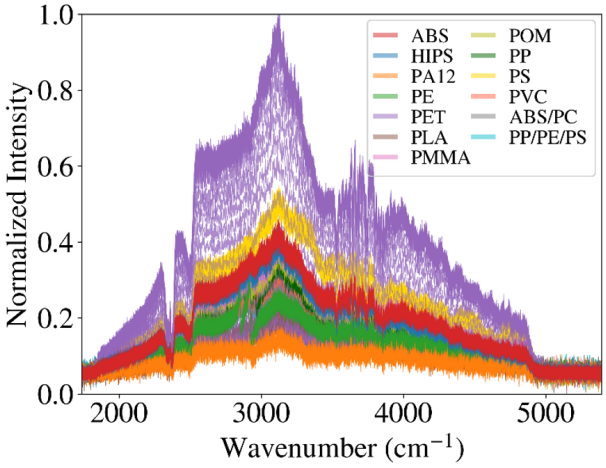

Figure 3: Normalized MIR spectra of various plastic materials.

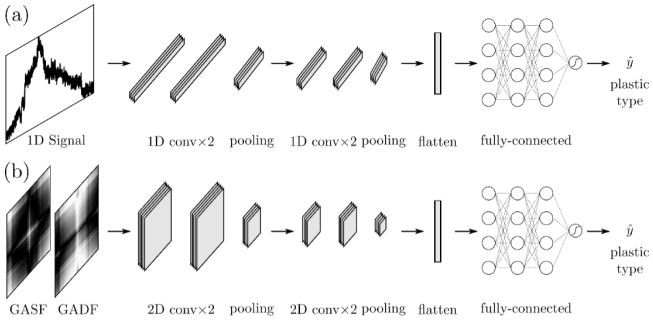

Figure 4: Architectures of (a) PlasticNet (1D) and (b) PlasticNet (2D). The plastic network (1D) inputs a spectrum vector and outputs the predicted plastic type.

a variety of operations. Gramian angular summation fields (GASF) and Gramian angular difference fields (GADF) are the two different types of GAFs. Each component of GASF and GADF is the cosine of the angle sum and the sine of the angle difference, respectively. Normalizing IR spectra to a value between 0 and 1 is the initial step in constructing the GAF matrix. The second step following normalization is to represent the normalized vector $\hat{x}$ in polar coordinates using the following transformations:

$$\phi_i = \arccos(\hat{x}_i),\ i = 1, \cdots, n \tag{2}$$

$$r_i = \frac{i}{n},\ i = 1, \cdots, n \tag{3}$$

where i is the index of the n-dim vector entry; $\phi \in \mathbb{R}^n$ is the angle vector, and $r \in \mathbb{R}^n$ is the radius vector. Finally, the GASF and GADF matrices are obtained as

$$\text{GASF} = \cos(\phi_i + \phi_j) = \hat{x}^T \hat{x} - \sqrt{I - \hat{x}^2}^T \sqrt{I - \hat{x}^2} \tag{4}$$

$$\text{GADF} = \sin(\phi_i - \phi_j) = \sqrt{I - \hat{x}^2}^T \hat{x} - \hat{x}^T \sqrt{I - \hat{x}^2} \tag{5}$$

where $I = [1, \cdots, 1]$ is a univer row vector of size n. Although the resulting GASF and GADF matrices are dense and large,

they can be reduced using the piecewise aggregation approximation (PAA) method [18]. Fig. 5 depicts the conversion of spectra to GASF and GADF matrices. The matrices are represented as grayscale images.

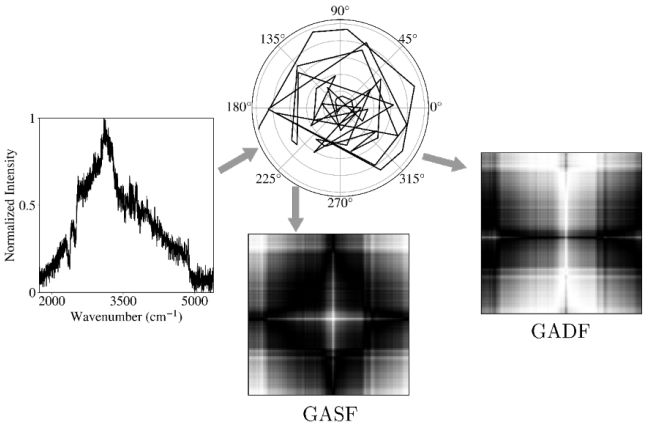

Figure 5: Conversion from 1D signal to GASF and GADF matrices. The 1D signal is first mapped to the polar coordinate system and finally converted to GASF and GADF matrices. Encoding the 1D signal into GAF matrices captures the relationship between the signal intensity at different wavenumbers.

2D CNN

2D CNNs are commonly used to classify images, which are multichannel matrices (tensor). For example, 2D CNNs are usually used to classify RGB images (each channel is a color channel). In our method, we use a two-channel data representation with the GASF and GADF matrices as channel embeddings. The size of the input varies from $25 \times 25 \times 2$ to $200 \times 200 \times 2$, depending on the scale of the PAA reduction. The 2D convolution operation looks for meaningful patterns from GASF and GADF matrices. The two-channel GASF/GADF object is fed into a 2D CNN, which we refer to as PlasticNet (2D). PlasticNet (2D) contains four 2D convolutional layers, two 2D max-pooling layers, and three fully connected layers (Fig. 4). The 2D convolutional layer has 64 filters of size 3×3, and the 2D max-pooling layer has filters of size 2×2. The setups for all hyperparameters are the same as those used in PlasticNet (1D).

Saliency Analysis

Saliency maps are commonly employed to highlight features in the input data that are deemed pertinent to the predictions of a CNN model. In our case, these techniques attempt to emphasize aspects of the specific object of input data that the CNN is searching for. Among all saliency map methods, the most theoretically complete is the integrated gradient (IG) method [19, 20]. For the PlasticNet (2D) case, let $V \in \mathbb{R}^{100\times100\times2}$ be the input and θ be the parameter vector, the CNN can be written as a large and complicated equation complicated equation $F(V;\theta) : \mathbb{R}^{100\times100\times2} \to \mathbb{R}^c$, where output is the classification probability of c types of plastics. The loss function is then $L(F(V;\theta)) : \mathbb{R}^c \to \mathbb{R}$. The saliency map $S \in \mathbb{R}^{100\times100\times2}$ calculated by the IG as

$$S = \text{abs}\left((V - \bar{V}) \cdot \int_0^1 \frac{\partial L(\bar{V} + \beta(V - \bar{V};\theta))}{\partial V} d\beta\right) \tag{6}$$

where $\bar{V} \in \mathbb{R}^{100\times100\times2}$ is a baseline input that represents the absence of a feature in the input V and only contains zero values typically.

Results and Discussion

Classification results for ATR-FTIR and MIR data are presented in Fig. 6 and 7, respectively, along with comparisons of different input sizes.

For ATR-FRIR data, PlasticNet (2D) with an input size of $200 \times 200 \times 2$ has the highest accuracy of 87.29%. Support vector machine has a comparable accuracy of 86.14%. The accuracy of PlasticNet (2D) is always higher than that of PlasticNet (1D), indicating that the conversion from the original 1D signal to 2D GAF matrices captures more information. The accuracy of PlasticNet (2D) increases as the input matrix increases, indicating that a larger input matrix contains more information.

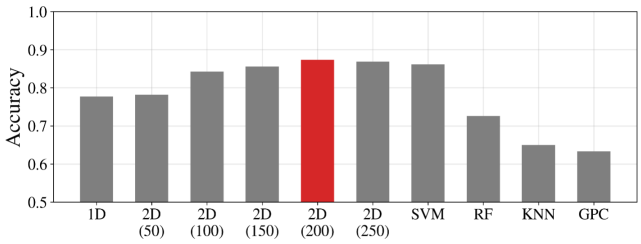

Figure 6: Comparison of the accuracy of CNN-based methods and other ML algorithms for ATR-FTIR data.

For MIR data, PlasticNet (1D) and (2D) with an input size of $100 \times 100 \times 2$, and K-nearest neighbor all have 100% accuracy. The red bars represent perfect classification accuracy. The accuracy of PlasticNet (2D) increases as the input matrix increases, indicating that a larger input matrix contains more information. However, using only 78% of the 1D data volume, PlasticNet (2D) with an input size of $25 \times 25 \times 2$ can still achieve 99.2% accuracy. This facilitates faster prediction and less memory requirements for plastic networks. Specifically, the prediction time for a single spectrum is about 121 μs ($\sim$8200 Hz), which is only 58% of the time for 1D CNN (208 μs, $\sim$4800 Hz). All CNN methods have sufficiently fast prediction rates compared to the fast MIR readout rate of 200 Hz in our measurements. Table 1 provides a comparison of the overall accuracy obtained with all CNN architectures explored as well as prediction time for a single spectrum.

For MIR data, we also performed a multilabel classification to determine the constituent plastic components in binary (ABS/PC) and ternary (PP/PE/PS) blends. For the binary blend, the algorithm predicted that it contained 99.8% ABS and 99.7% PC. For the ternary blend, it predicted that it contained 100% PE, PP, and PS and no other components.

To understand exactly what the CNNs have learned from the spectra, we used saliency maps to find the most important

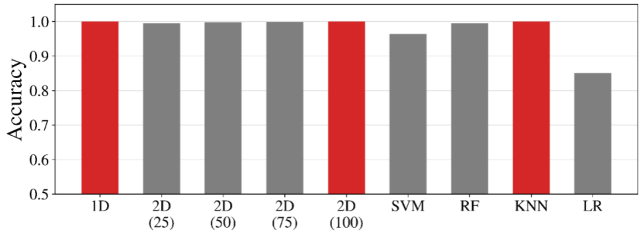

Figure 7: Comparison of the accuracy of CNN-based methods and other ML algorithms for MIR data.

Table 1: Overall Prediction Time Found with Different CNN Architectures and Other Machine Learning Models for MIR data.

	Prediction time (μs)
1D	208±5
2D (25×25)	121±7
2D (50×50)	300±5
2D (75×75)	361±3
2D (100×100)	1218±24
SVM	7188±31
RF	41±1
KNN	1564±8

regions for classification. For ATR-FTIR data, we used the results for PlasticNet (2D) with an input size of 200×200, since this has the highest accuracy. Fig. 8 shows the spectrum and its important regions of PE. The average saliency map for each plastic was studied because each spectrum has some subtle differences, and the common significant patterns were of interest. The darker regions in Fig. 8c are the most important ones. Specif- ically, the horizontal bands near 2900 cm^{-1} and vertical bands 2400 cm^{-1} were dark, which indicates the importance of the signal at these frequencies. Fig. 8d, shows the significant signal locations (shaded regions) and the raw spectrum. The bands between 2800 and 2900 cm^{-1} were of importance. This region provides characteristic IR bands for PE.

For MIR data, we used the results for PlasticNet (2D) with an input size of 100×100. Fig. 9 shows the spectrum and its important regions of ABS/PC. The darker regions in Fig. 9c are the most important ones. Specifically, the dark clusters have a horizontal location near 3200 and 3600 cm^{-1} and a vertical location near 3600 cm^{-1}, which indicates the importance of the signal at these frequencies. Fig. 9d, shows the significant signal locations (shaded regions) and the raw spectrum. The bands between 2700 and 3000 cm^{-1} and between 3200 and 3600 cm^{-1} were of importance.

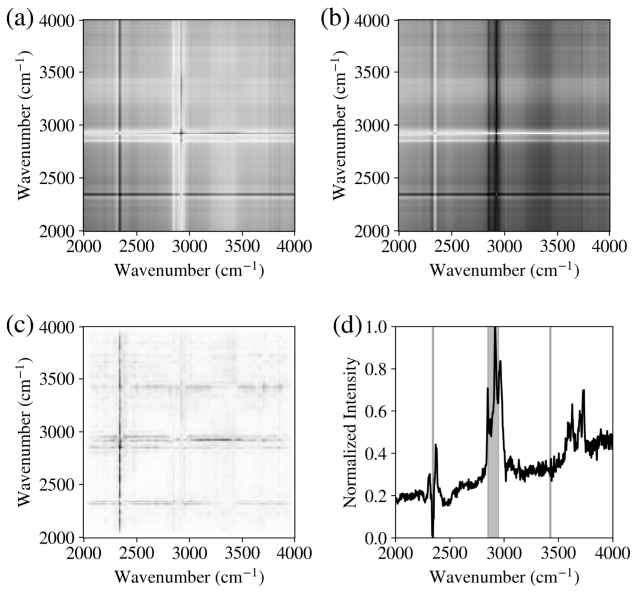

Figure 8: aliency analysis for PE. The average (a) GASF and (b) GADF matrices of size 200×200, where darker colors represent larger values. (c) The average saliency map of size 200×200. The darker regions are the most important regions for classification. (d) The average IR spectrum and the most important signals, shaded in gray. The most important region includes the bands between 2800 and 2900 cm^{-1}, which are the characteristic IR peaks of the PC.

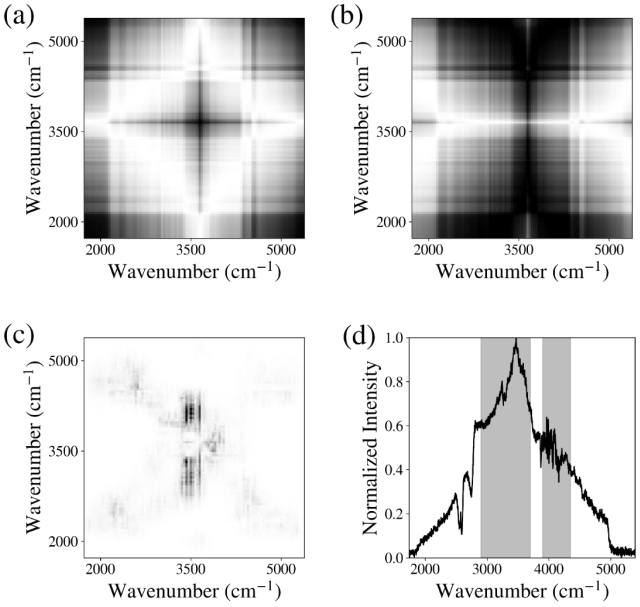

Figure 9: Saliency analysis for ABS/PC. The average (a) GASF and (b) GADF matrices of size 100×100, where darker colors represent larger values. (c) The average saliency map of size 100×100. The darker regions are the most important regions for classification. (d) The average IR spectrum and the most important signals, shaded in gray. The most important region includes the bands between 2700 and 3000 cm^{-1} and between 3200 and 3600 cm^{-1}.

Conclusion

convolutional neural network (CNN) framework for classifying different types of plastic materials that are commonly found in MPW based on ATR-FTIR and fast MIR spectra was developed. An important aspect of this type of spectral data is that it can be collected in real-time; as such, this approach provides an avenue for the high-throughput characterization of MPW. The proposed CNN framework (which

we call PlasticNet) uses a Gramian angular representation of the IR spectra and we show that this approach reaches overall classification accuracies of 87% for ATR-FTIR data and 100% for MIR data. The frame can identify not only pure plastics but also colored plastics and multiplastic blends. In addition, the CNN framework had a fast prediction rate compared to other ML methods, matching the readout rate of fast MIR. This allows us, in the future, to build software to automatically acquire high-throughput IR data and combine it with CNN to predict the plastic composition in real time.

References

[1] EPA. *Advancing Sustainable Materials Management: 2018 Fact Sheet Assessing Trends in Material Generation and Management in the United States*, 2020.

[2] PO Awoyera and Adeyemi Adesina. Plastic wastes to construction products: Status, limitations and future perspective. *Case Studies in Construction Materials*, 12:e00330, 2020.

[3] Sathish Paulraj Gundupalli, Subrata Hait, and Atul Thakur. A review on automated sorting of source-separated municipal solid waste for recycling. *Waste management*, 60:56–74, 2017.

[4] N Kiran, E Ekinci, and CE Snape. Recyling of plastic wastes via pyrolysis. *Resources, Conservation and Recycling*, 29(4):273–283, 2000.

[5] Long Yu, Katherine Dean, and Lin Li. Polymer blends and composites from renewable resources. *Progress in polymer science*, 31(6):576–602, 2006.

[6] Daniel Jose da Silva and Helio Wiebeck. Current options for characterizing, sorting, and recycling polymeric waste. *Progress in Rubber, Plastics and Recycling Technology*, 36(4):284–303, 2020.

[7] Charles Signoret, Anne-Sophie Caro-Bretelle, José-Marie Lopez-Cuesta, Patrick Ienny, and Didier Perrin. Mir spectral characterization of plastic to enable discrimination in an industrial recycling context: Ii. specific case of polyolefins. *Waste Management*, 98:160–172, 2019.

[8] Mohammad N Siddiqui, Mohammad A Gondal, and Halim H Redhwi. Identification of different type of polymers in plastics waste. *Journal of Environmental Science and Health, Part A*, 43(11):1303–1310, 2008.

[9] Charles Signoret, Anne-Sophie Caro-Bretelle, José-Marie Lopez-Cuesta, Patrick Ienny, and Didier Perrin. Alterations of plastics spectra in mir and the potential impacts on identification towards recycling. *Resources, Conservation and Recycling*, 161:104980, 2020.

[10] Qi Wu, Fengming Yu, Yoji Okabe, Kazuya Saito, and Satoshi Kobayashi. Acoustic emission detection and position identification of transverse cracks in carbon fiber–reinforced plastic laminates by using a novel optical fiber ultrasonic sensing system. *Structural Health Monitoring*, 14(3):205–213, 2015.

[11] Wartini Ng, Budiman Minasny, Maryam Montazerolghaem, Jose Padarian, Richard Ferguson, Scarlett Bailey, and Alex B McBratney. Convolutional neural network for simultaneous prediction of several soil properties using visible/near-infrared, mid-infrared, and their combined spectra. *Geoderma*, 352:251–267, 2019.

[12] Xiaoyi Chen, Qinqin Chai, Ni Lin, Xianghui Li, and Wu Wang. 1d convolutional neural network for the discrimination of aristolochic acids and their analogues based on near-infrared spectroscopy. *Analytical Methods*, 11(40):5118–5125, 2019.

[13] Shengli Jiang, Zhuo Xu, Medhavi Kamran, Stas Zinchik, Sidike Paheding, Armando G McDonald, Ezra Bar-Ziv, and Victor M Zavala. Using atr-ftir spectra and convolutional neural networks for characterizing mixed plastic waste. *Computers & Chemical Engineering*, 155:107547, 2021.

[14] Stas Zinchik, Shengli Jiang, Søren Friis, Fei Long, Lasse Høgstedt, Victor M Zavala, and Ezra Bar-Ziv. Accurate characterization of mixed plastic waste using machine learning and fast infrared spectroscopy. *ACS Sustainable Chemistry & Engineering*, 9(42):14143–14151, 2021.

[15] Wolfgang Becker, Kerstin Sachsenheimer, and Melanie Klemenz. Detection of black plastics in the middle infrared spectrum (mir) using photon up-conversion technique for polymer recycling purposes. *Polymers*, 9(9):435, 2017.

[16] Armin Lambrecht, Carsten Bolwien, Johannes Herbst, Frank Kühnemann, Vincenz Sandfort, and Sebastian Wolf. New methods of laser-based gas analysis. *Chemie Ingenieur Technik*, 88(6):746–755, 2016.

[17] Zhiguang Wang and Tim Oates. Encoding time series as images for visual inspection and classification using tiled convolutional neural networks. In *Workshops at the twenty-ninth AAAI conference on artificial intelligence*, 2015.

[18] Eamonn J Keogh and Michael J Pazzani. Scaling up dynamic time warping for datamining applications. In *Proceedings of the sixth ACM SIGKDD international conference on Knowledge discovery and data mining*, pages 285–289, 2000.

[19] Mukund Sundararajan, Ankur Taly, and Qiqi Yan. Axiomatic attribution for deep networks. In *International conference on machine learning*, pages 3319–3328. PMLR, 2017.

[20] Julius Adebayo, Justin Gilmer, Michael Muelly, Ian Goodfellow, Moritz Hardt, and Been Kim. Sanity checks for saliency maps. *Advances in neural information processing systems*, 31, 2018.